Diurnal Variability of Regional Cloud and Clear-Sky Radiative Parameters Derived from GOES Data. Part II: November 1978 Cloud Distributions

PATRICK MINNIS AND EDWIN F. HARRISON

Atmospheric Sciences Division, NASA Langley Research Center, Hampton, VA 23665

(Manuscript received 8 November 1982, in final form 23 March 1984)

ABSTRACT

Regional (250×250 km^2) diurnal cloud variability is examined using mean hourly cloud amounts derived from November 1978 GOES-East visible and infrared data with a hybrid bispectral threshold technique. A wide variety of diurnal variations in cloud cover is presented. A morning maximum in low cloudiness is found over much of the eastern Pacific. Many regions in the western Atlantic have peak low-cloud cover near noon. Low clouds reach a maximum most often near noon over most of South America and in the morning over North America. Midlevel clouds are most frequent in the evening over oceans and in the early morning over land. High-cloud maxima are found mainly in the late afternoon over land and in the midafternoon over the oceans. An early morning minimum in high-cloud-top temperature is observed over marine areas. The amplitude of the semidiurnal component of cloudiness is generally much less than that of the diurnal component.

The largest diurnal cloud variations occur over the southeastern Pacific where low clouds are dominant. On the average, mean cloud fraction varied by about 0.35 in this area with a maximum near sunrise. Over the Amazon Basin, the vertical distribution of cloud cover follows a pronounced diurnal cycle which shows maximum high-cloud cover occurring in the late afternoon. A large-scale diurnally modulated circulation feature between the Amazon and the adjacent oceans is suggested. High clouds occur most frequently over the southern Andes during the afternoon and are most common over the adjacent lowlands during the night, indicating the existence of a diurnally-dependent mountain–plains circulation.

1. Introduction

A first step toward fully understanding the role of clouds in the Earth's climate is increasing our knowledge of the temporal and spatial variability of the amounts, types and radiative properties of clouds. One important time scale of cloud variability which is not adequately understood or documented is the 24-hour solar or diurnal cycle (Minnis and Harrison, 1984a). Cloudiness is involved in a number of physical processes (e.g., radiative exchange, precipitation, small- and large-scale dynamics) in the atmosphere. Therefore, these processes will have diurnal components if cloud cover varies on a 24-hour basis. Increased knowledge of diurnal cloud variability should lead to a better understanding of the complex mechanisms involving clouds.

Several recent investigations have noted the role of diurnal cloud variations in several atmospheric processes. In some tropical areas, it has been determined that the oscillations of clouds on a daily basis are part of a dynamic-radiative feedback mechanism (Ackerman and Cox, 1981) which may operate on various spatial scales (Foltz and Gray, 1979). Daily cycles of cloud growth and dissipation within tropical ocean cloud clusters correspond to the diurnal cycles in heavy convective rainfall reported by Ruprecht and Gray (1976) and many others. Browner *et al.* (1977) found an inverse relationship between the intensity of a tropical storm and the diurnal oscillation of its cirrus canopy. Brier and Simpson (1969) established a statistical relationship between tropical cloudiness, rainfall and the semidiurnal solar atmospheric tide which is manifested in semidiurnal variations of surface pressure.

Diurnal variations in cloud cover over the GARP Atlantic Tropical Experiment (GATE) A/B scale array have been measured by a number of researchers and utilized for a variety of purposes. Gruber (1976) found a semidiurnal oscillation in cloudiness for the A/B area which may be an indication of an atmospheric tidal effect. McGarry and Reed (1978) found some relationships between the local times of maximum convective cloud cover and maximum rainfall rates. Diurnal cloud data derived by Cox and Griffith (1979) were used in their estimation of GATE Phase III radiative divergence profiles. Using cloud cover characteristics also derived from GATE data, Ball *et al.* (1980) were able to differentiate various diurnal cycles in the A/B region. They concluded that diurnal variations of cloudiness are highly dependent on regional location and the prevalent convective activity. Therefore, generalizations about diurnal cloud variations may be applicable only to a specific portion of

the globe during a particular season. This conclusion highlights the need for monitoring cloud cover at spatial and temporal scales sufficient to account for seasonal and regional changes in diurnal cloud variability.

There is also evidence of significant diurnal cloud variations in many extratropical regions. Wallace (1975) documented significant diurnal variations in thunderstorm activity over the United States. Simon (1977) found a strong diurnal cycle in low cloudiness off the coast of California. Short and Wallace (1980) inferred cloudiness from averaged morning and evening measurements of infrared radiation taken from the National Oceanic and Atmospheric Administration (NOAA) satellites. In addition to large diurnal cloud variations over tropical areas, their results indicate substantial diurnal changes in cloudiness over some continental and oceanic areas in the middle latitudes. This paper documents the diurnal variations in low, middle, high and total cloudiness and cloud-top temperatures derived from hourly geostationary satellite data.

2. Data and analysis

The cloud results reported here were derived from November 1978 Geostationary Operational Environmental Satellite (GOES) visible and infrared data. Minnis and Harrison (1984a) give a detailed account of the input GOES data and the cloud-quantification algorithm. Mean total cloud amount for November 1978 was computed for each region in a staggered, equal-area (250 × 250 km^2) grid encompassing the area between 45°N and 45°S latitudes and 30 and 125°W longitudes. This quantity is

$$\bar{C} = \sum_{i=1}^{24} C(t_i)/24, \tag{1}$$

where t_i is some local time, $C(t_i)$ the monthly average cloudiness at t_i, and i increments t by 1 h. The mean total cloud amount is the sum of the mean low, middle and high cloud fractions, $\bar{C}_1$, $\bar{C}_2$ and $\bar{C}_3$, respectively, which are also found from hourly quantities as in (1). Cloud level is determined from the 11.5 μm (IR) equivalent blackbody temperature T of a given cloudy pixel (Minnis and Harrison, 1984a) as follows. Cloud level is

$$\begin{aligned} &\text{low for} && T \geqslant \bar{T}_s - 13, \\ &\text{midlevel for} && \bar{T}_s - 13 > T \geqslant \bar{T}_s - 39, \\ &\text{and high for} && T < \bar{T}_s - 39, \end{aligned}$$

where $\bar{T}_s$ is the 24-hour average of the clear-sky IR equivalent blackbody temperature. These temperature thresholds roughly correspond to altitude ranges of 0 to 2 km, 2 to 6 km and greater than 6 km for low, middle and high clouds, respectively, assuming a lapse rate of −6.5 K km^{-1}. All quantities associated with low, middle and high clouds are denoted with the subscripts 1, 2 and 3 respectively. Overbars denote 24-hour monthly means. Their absence indicates hourly monthly means. Average cloud-top temperature, $\bar{T}_c$, is the average IR equivalent blackbody temperature of C. The mean diurnal range in $\bar{C}$ is

$$\Delta C = C(t_{\max}) - C(t_{\min}), \tag{2}$$

where $t_{\max}$ and $t_{\min}$ are the local times of maximum and minimum cloudiness respectively. The normalized diurnal range in cloudiness is $\Delta N = \Delta C/\bar{C}$. A harmonic analysis was performed on normalized hourly cloud fractions, $N(t_i) = C(t_i)/\bar{C}$, to determine the phase and amplitude of the diurnal S_1 and semidiurnal S_2 components of each quantity.

3. Results

The volume of data resulting from this analysis precludes detailed discussion of clouds in all regions. Therefore, a brief summary of all of the results will be presented first followed by a closer examination of some of the more prominent features. Figs. 1a–d show the distributions of $\bar{C}$, $\bar{C}_1$, $\bar{C}_2$ and $\bar{C}_3$. Much of the eastern Pacific extending from the western edge of the grid between 5°N and 20°S to the coast of South America between 5°N and 30°S is dominated by low-level clouds (Fig. 1b). Total cloud cover (Fig. 1a) for this area, greatest around 15°S and 85°W, diminishes rapidly toward the coast and gradually in all other directions before giving way to several different cloud regimes. From the GOES imagery, it is apparent that the clouds in the area of greatest cloudiness are mostly stratus (St) and stratocumulus (Sc). The decreasing cloud amounts toward the west are consistent with the observations of Agee *et al.* (1973) that the clouds change from the closed cell (high cloud fraction, e.g., Sc) to open cell types (lower cloud amounts) from east to west in this area of the Pacific. The cloud cover decreases gradually to the north from the center of the low cloud zone, then increases rapidly at the equator. Middle and high clouds associated with the intertropical convergence zone (ITCZ) are more common north of 5°N. The ITCZ, centered along 12°N, covers about 10° of latitude over the eastern Pacific with $\bar{C} > 0.5$ and $\bar{C}_3 > 0.1$. This transition from St to Sc to trade cumulus (Cu) to the high clouds of the ITCZ conforms well with the idealized depiction of the Hadley circulation given by Schubert (1976). Significant levels of middle and high clouds are also found over the area centered along a line from 25°S at 120°W to 40°S at 90°W south of the Sc zone. This line is near the mean position of the southern polar front.

The cloudiness over the Pacific north of 25°S is consistent with the long-term mean given by Sadler *et al.* (1976). An exception to this general agreement

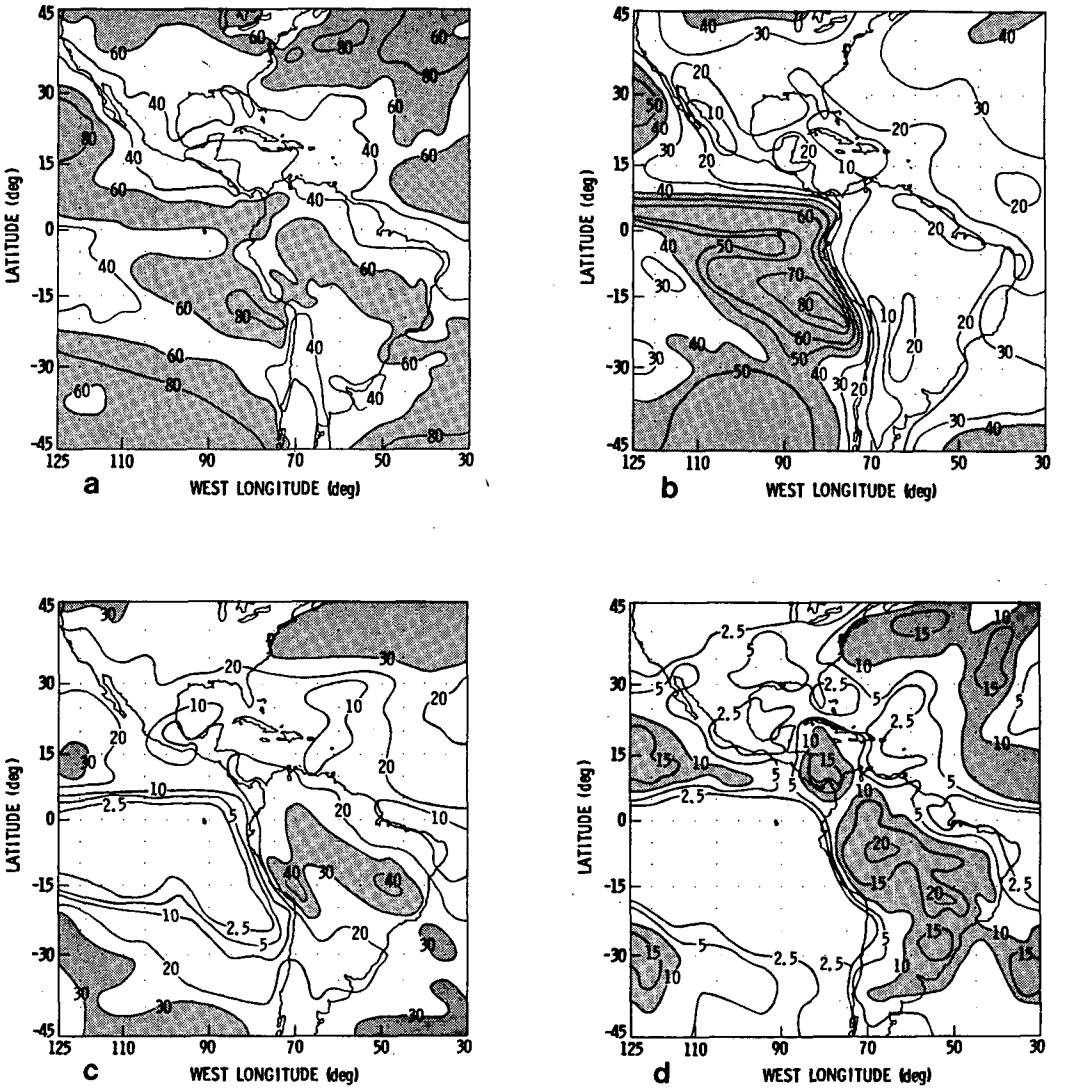

FIG. 1. Mean cloud fraction (in percent) for (a) total cloud cover, (b) low cloud, (c) midlevel cloud and (d) high cloud for November 1978.

is the cloudiness over the area west of Mexico where $\bar{C} > 0.75$. It is similar to the large cloud anomaly found by Sadler *et al.* (1976) for November 1975. This region corresponds to the position of the mean November 1978, 700 mb trough (Dickson, 1979). Deserts and adjacent marine areas near both the North and South American Pacific coasts have total cloudiness less than 0.40 composed of a mix of cloud types. Regions in the Gulf of Mexico and adjoining Atlantic also have low total cloudiness composed mostly of low-level clouds.

Over the central and eastern United States, $\bar{C}$ cloud amount is generally greater than 0.50 with high-level clouds comprising a significant portion of the total cloud cover only in the south and over the east coast. The use of a -6.5 K km^{-1} lapse rate may have caused an underestimation of high- and middle-level cloudiness in the northern part of this area. Typical midlatitude wintertime lapse rates are approximately -3.5 K km^{-1} in the lower 4 km of the atmosphere. Midlevel cloudiness is the most significant type over western North America.

Cloud cover over the North Atlantic is generally greater than 0.50 and comprised of cloudiness at all levels. Two other portions of the ITCZ are evident over the Atlantic Ocean northeast of South America and over the Caribbean Sea at about 12°N. The clouds here are primarily at the high and middle levels. Northeastern Brazil and the lower Amazon Basin have low levels of total cloudiness, which correspond to the precipitation minima usually found in these areas during November (Trewartha, 1968).

The area of heavy cloud cover south of this region usually has no dry season. It is part of a much larger area of heavy cloud cover which extends from Panama through southeastern Brazil and well into the South Atlantic along the mean low-level northwesterly flow. The percentages of high and middle cloud amounts are quite significant in this area.

The mean diurnal ranges or amplitudes and times of maximum cloudiness are presented in vectorial form. The value of t_{max} is represented by the direction of an arrow (defined by the bare end of the arrow) on a 24 h clock. Local midnight is given by an arrow pointing straight up (bare end at top), while local noon is indicated by a vector pointing straight down. Arrows pointing to the right or left indicate 0600 Local Time (LT) or 1800 LT respectively. The magnitude of the range or amplitude is given by the number of barbs and the size of the box. The values of the barbs and boxes are 0.1 and 0.25 respectively. A barb or half barb is plotted on one side of the arrow while the boxes are plotted on the opposite side to achieve the specified magnitude. For example, the arrow on the left in Fig. 2 indicates that t_{max} = 1500 LT and the amplitude is 0.1. The vector in the center shows that t_{max} = 0600 LT and the amplitude is 0.40 (one and a half barbs and one box). On the right is a vector showing t_{max} = 0000 LT and a diurnal amplitude of 0.85 (one barb and three boxes).

Figure 3 presents the values of t_{max} and the diurnal *ranges* of total, low, middle and high cloudiness for every other region. Results are given for those areas where the mean cloud fraction at a given level is greater than 0.01 and the range exceeds a certain value. Areas where the diurnal cloud variations are not statistically significant at the 0.95 confidence level (according to the Fisher *F*-test) are shaded. These regions are shown because they are included in the discussion and some significant conclusions may be drawn when these regions are considered together. It is apparent from this figure that the areas with the greatest values of ΔC are confined mainly to the southern tropics. The most substantial diurnal ranges in total cloudiness occur over the eastern Pacific where low clouds are the dominant feature. In this area, Figs. 3a and 3b are identical; maximum cloudiness, C_{max} occurs around 0600 LT over most of the regions. Over South America, C_{max} occurs at various times of day. Mean maximum total cloud cover is observed primarily in the hours near sunrise over North America and near noon over much of the Atlantic north of 25°N. Maximum cloudiness is commonly seen over much of the ITCZ between 1200 and 1500 LT.

The diurnal variations in low cloud cover (Fig. 3b) appear to have more spatial homogeneity than those seen for total cloudiness. For example, low clouds peak near local noon over much of South America and between 0300 and 0900 LT over most of the eastern Pacific and North America. Midday low-cloud maxima are also relatively frequent over the western North Atlantic and in the ITCZ. The largest values of ΔC_1 are found between 5°N and 25°S latitudes.

Diurnal variations in middle cloudiness also show some large-scale homogeneities. Middle cloud maxima occur during the late afternoon and early evening near the northeastern coast of South America and during the late evening and early morning hours over much of the remainder of the continent. Peak values of C_2 are seen around 1800 LT over many of the ITCZ regions in the Pacific and over many other regions in the Pacific where $\bar{C}_2$ is significant. In most other areas of the grid, midlevel cloudiness shows a nocturnal maximum.

Figure 3d shows that high clouds undergo some very substantial diurnal variations, especially over continental areas. Over most of South America north of 20°S, C_{3max} occurs in the late afternoon and early evening. South of this latitude, the time of maximum high-cloud cover appears to vary longitudinally: near 1500 LT over the Andes, during the night over the lowlands to the east and near 1800 LT over the Brazilian Highlands. Over North America, the Gulf of Mexico, the Caribbean Sea, the South Atlantic and the North Pacific, high clouds reach maximum coverage during the afternoon (1200 to 1800 LT) in nearly 70% of the areas where the diurnal cycle is significant. Peak high cloudiness occurs in the afternoon over 50% of the regions in the South Pacific and North Atlantic Oceans. The times of C_{3max} are distributed fairly uniformly for the remainder of the oceanic regions.

Values of $\bar{T}_c$, shown in Fig. 4, are generally consistent with the combination of three levels of cloudiness given in Fig. 1. Some exceptions may be found over North America where $\bar{T}_c$ is generally lower than it is over adjacent ocean areas, although $\bar{C}_3$ is much greater over the latter. This difference may be ascribed to differences in the values of T_s (Minnis and Harrison, 1984a) which initialize the lapse rate used to define the cloud altitude. The clear-sky temperatures over the United States during this time period were from

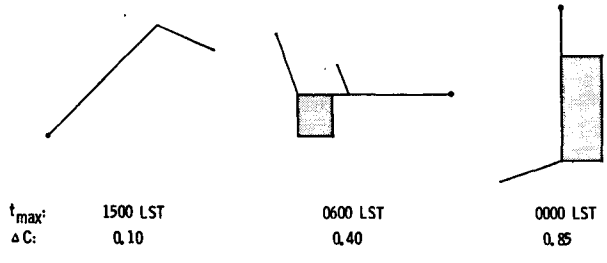

FIG. 2. Examples of phase and amplitude plotting conventions. One full barb equals 0.1 units and one box equals 0.25 units.

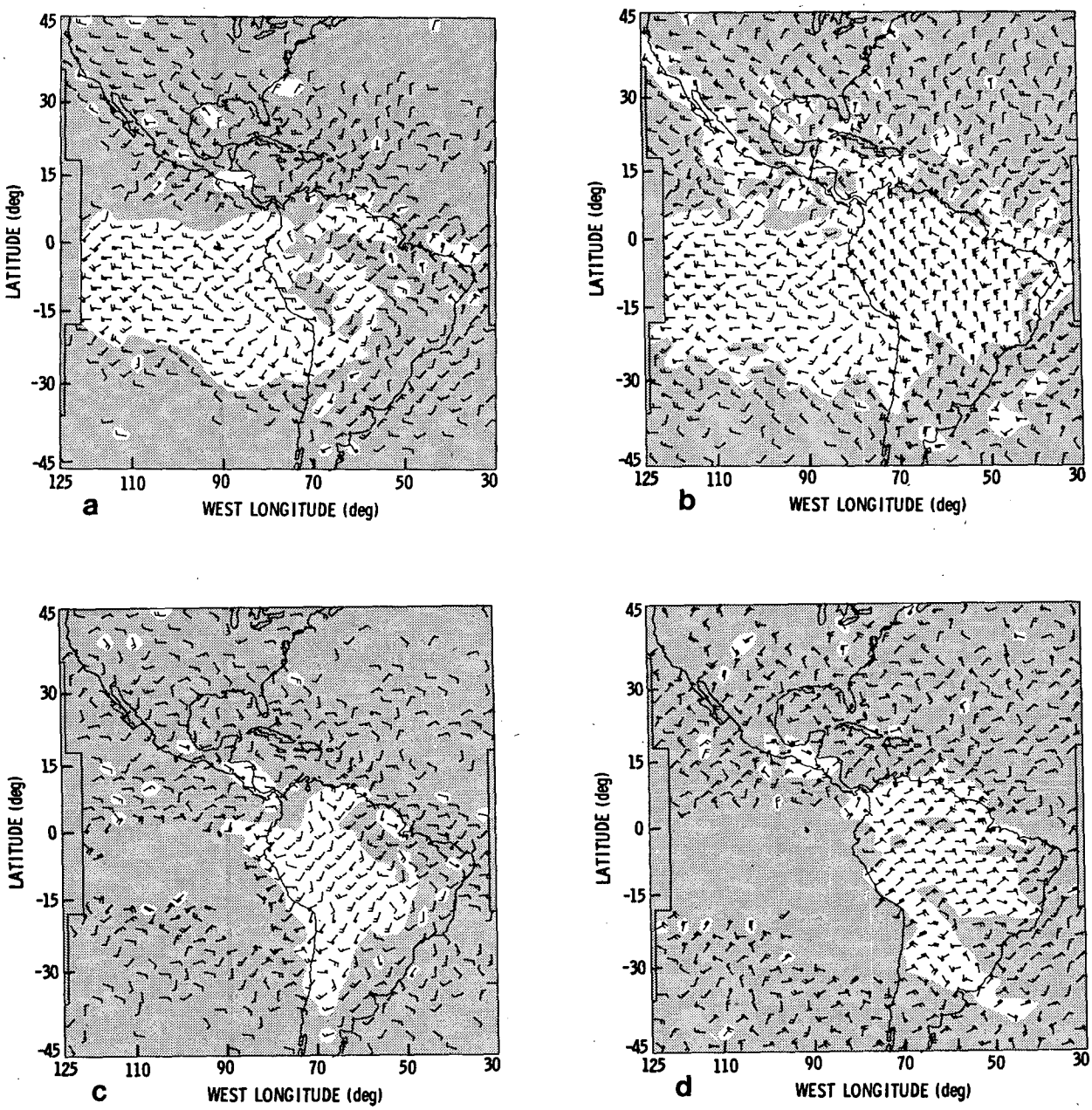

FIG. 3. Normalized diurnal *range* and phase of (a) total cloud cover, (b) low cloud cover, (c) midlevel cloud cover and (d) high cloud cover for November 1978 using plotting convention of Fig. 2. Only ranges ≥0.1 are plotted. Unshaded areas are statistically significant at the 0.95 confidence level.

5 to 10 K less than those over the Atlantic Ocean at the same latitude (Minnis and Harrison, 1984b). Thus, the high-cloud temperature thresholds over the continent are 5 to 10 K lower than over the adjacent oceans. This effect and the use of a common lapse rate for all latitudes may cause some underestimation of middle- and high-level cloudiness over the United States. Over the western United States, the low values of $\bar{T}_c$ are due to higher surface elevation and to the mean position of the 750 mb trough. Colder cloud-top temperatures ($\bar{T}_c < 260$ K) are also found over areas of persistent deep convection south of 20°N. Areas with relatively warm cloud-top temperatures ($\bar{T}_c > 280$ K) generally correspond closely to those areas where low clouds are predominant.

The distribution of the diurnal ranges in cloud-top temperature ΔT_c is given in Fig. 5. This plot summarizes, to some extent, the diurnal regularity of the changes in the vertical distribution of clouds over a given region. The greatest values of ΔT_c are found

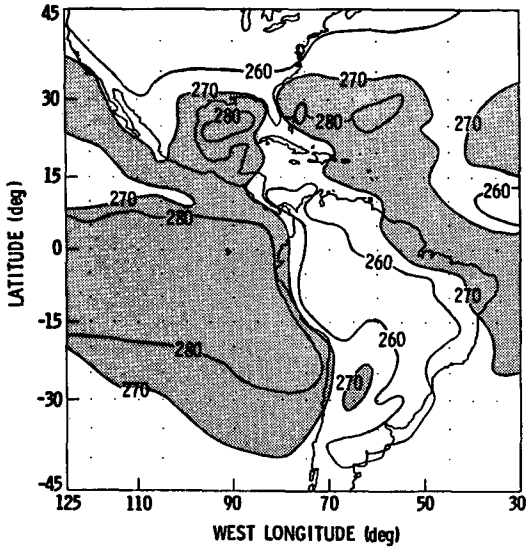

FIG. 4. Mean cloud-top temperature in Kelvin units for November 1978.

over South America where ΔC_3 is highest. Some exceptions include desert areas, such as the Andean Altiplano where the diurnal variations in T_c may be the result of surface effects. Intermediate values (5–15 K) of ΔT_c are found over the ITCZ and southern North America, where moderate diurnal variations in middle and high cloudiness are observed. The areas of lowest ΔT_c include regions with minimal diurnal variations in $\bar{C}_2$ and $\bar{C}_3$, areas where diurnal variations in $\bar{C}_2$ and $\bar{C}_3$ are out of phase and regions containing mostly low clouds.

Results of the harmonic analysis of mean low- and high-cloud cover are shown in Figs. 6 and 7 respectively. Diurnal and semidiurnal phase and *amplitude* arrows are given in each figure. The orientations of the arrows give the phases of both semidiurnal maxima. In Fig. 2, for example, the orientation of the arrow on the left would indicate maxima at 0300 LT (barb end) and 1500 LT (bare end), if it were used for the semidiurnal component. The phase and amplitude of the diurnal component from the harmonic analysis are plotted in these figures since they are not always identical to those for the observed diurnal range in Fig. 3. For example, the low-cloud diurnal component maxima $S_1(C_1)$ in Fig. 6a over South America occur near 0900 LT over many regions where $C_{1\max}$ is observed near 1100 LT (see Fig. 3b). The low-cloud semidiurnal maxima $S_2(C_1)$ centered around midnight and noon over these same regions (Fig. 6b) are inconsistent with $S_1(C_1)$ and help explain $C_{1\max}$ near noon. Over the southeastern Pacific, the semidiurnal maxima at 0900 and 2100 LT lag the diurnal component peak at 0600 LT. The low-cloud semidiurnal phases around 0300 and 1500 LT are temporally consistent with the diurnal component over many regions in the west central Atlantic. In almost all cases in Fig. 6, the amplitude of the semidiurnal component is less than that of the diurnal component.

The harmonic components of the diurnal variations in C_3 also show some large-scale coherency (Fig. 7). Over much of South America, $S_1(C_3)$ and $S_2(C_3)$ are temporally inconsistent. The semidiurnal maxima around 0400 and 1600 LT and diurnal component phases between 1800 and 2000 LT yield $C_{3\max}$ around 1700 LT. Near the Atlantic coast, $S_2(C_3)$ shows late-evening and mid-morning maxima. The semidiurnal maxima occur within 3 hours of 0300 and 1500 LT over 75% of all ocean regions (Fig. 7b). The semidiurnal components for middle cloudiness (not shown) also have some large-scale patterns, but are generally smaller than those for C_3. The semidiurnal cycles for total cloud cover are not as significant as those for any given cloud level, except in those areas such as the southeastern Pacific where clouds at one level are clearly dominant.

a. Eastern Pacific low cloudiness

One of the more outstanding features in the previous figures is the vast area of low cloudiness over the southeastern Pacific (SEP). The cloud cover in this area follows a pronounced diurnal cycle, $\Delta C > 0.30$, which generally peaks around sunrise. Fig. 8 shows a typical example of the time variation of cloudiness over this area. From its maximum coverage before sunrise, the cloudiness dissipates gradually at first, then rapidly diminishes after 0900 LT until 1300 LT. Shortly before sunset, the cloud cover begins to increase until the next morning. Fig. 8 also

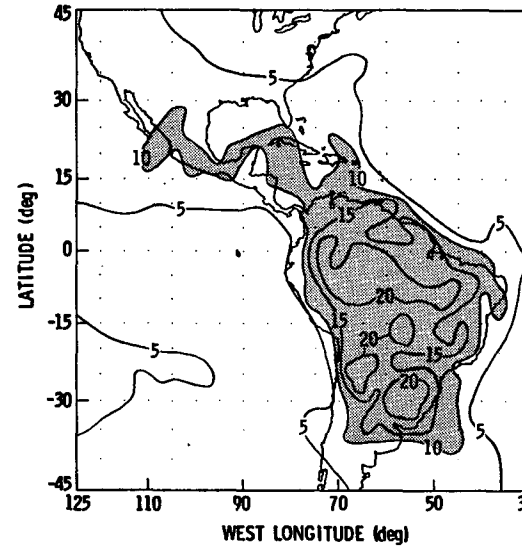

FIG. 5. Diurnal range of mean cloud-top temperature in Kelvin units for November 1978.

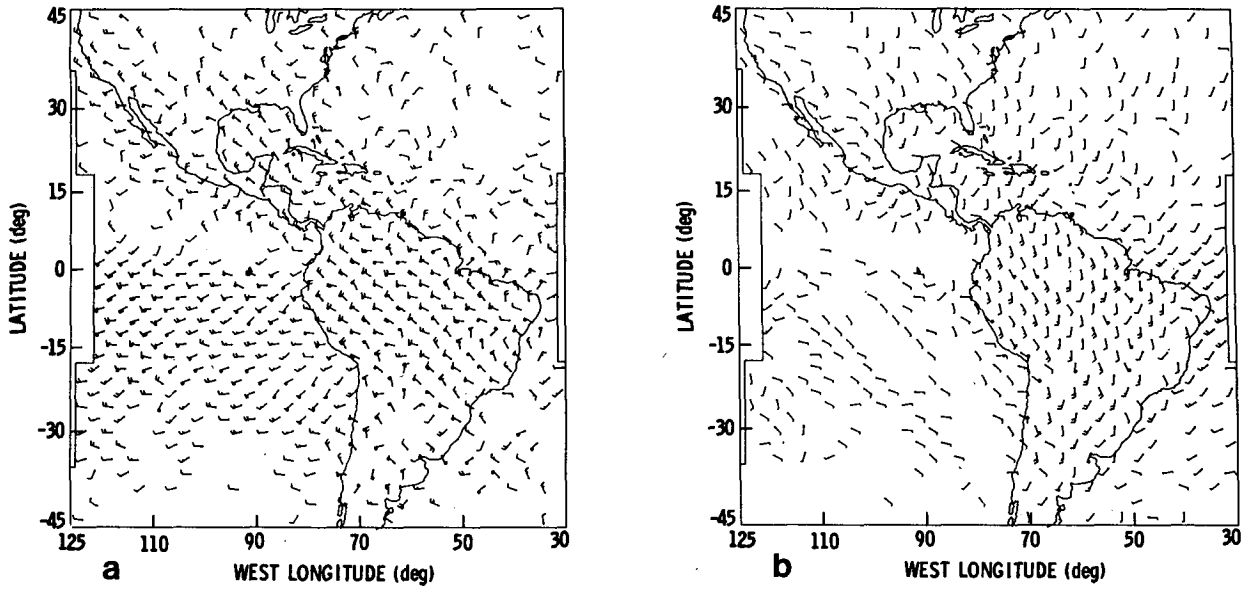

FIG. 6. (a) Phase and *amplitude* of diurnal component of normalized low-cloud cover from harmonic analysis for November 1978 using plotting convention of Fig. 2. (b) As in (a) except for semidiurnal component. Only amplitudes ≥0.05 are plotted.

shows the diurnal variation in T_c which is typical of the SEP low-cloud zone. As cloud cover increases, T_c decreases, while the opposite is true for decreasing cloudiness. This indicates that the cloud cover is probably thickening and the cloud top (top of boundary layer) is rising while the cloud cover builds, as suggested in Arakawa's (1975) illustration. The diurnal ranges of T_c over the entire Pacific low cloud zone are not very great (Fig. 6), although the phases of the diurnal variations in T_c over the zone are much the same as those in Fig. 8.

Figure 9 shows plots of cloudiness for 40 regions in the SEP to demonstrate the typicality of the cloud variations in Fig. 8. Each graph in Fig. 9 represents the diurnal variation of mean total cloudiness for a 250×250 km^2 region located between 9 and 18°S latitude and 99 and 76.5°W longitude. The plots on the right edge of the figure correspond to regions which include part of the Peruvian coast (top) or lie near it (bottom). Cloud variability is quite uniform in the left half of the figure with cloud amounts decreasing from north to south. Approaching the

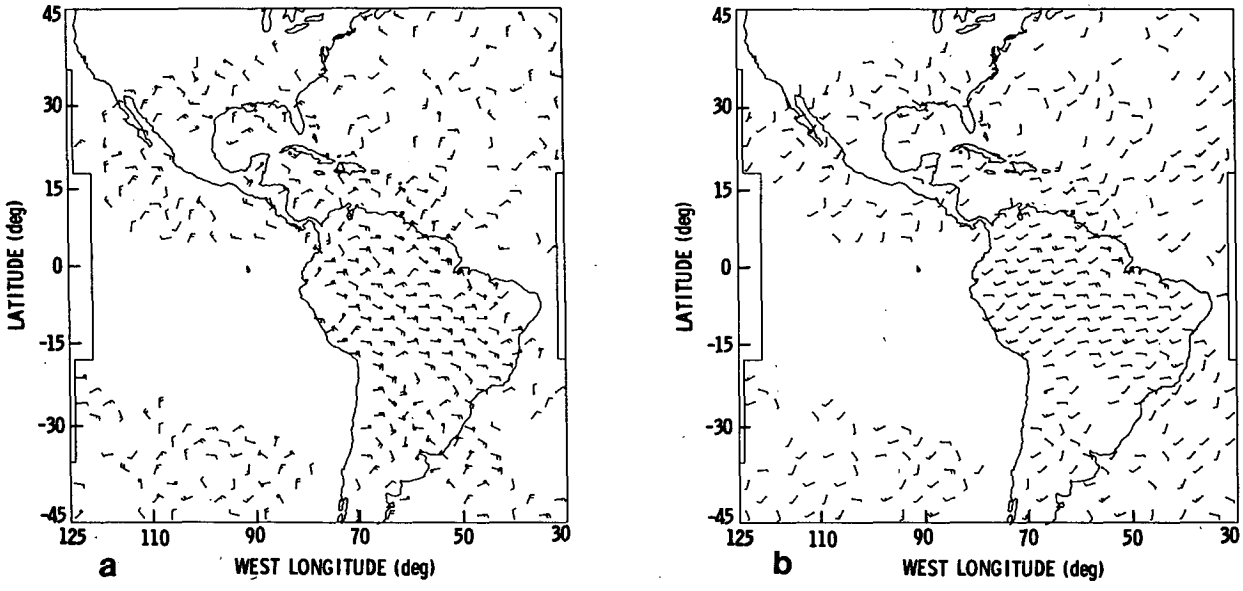

FIG. 7. As in Fig. 6 except for high clouds.

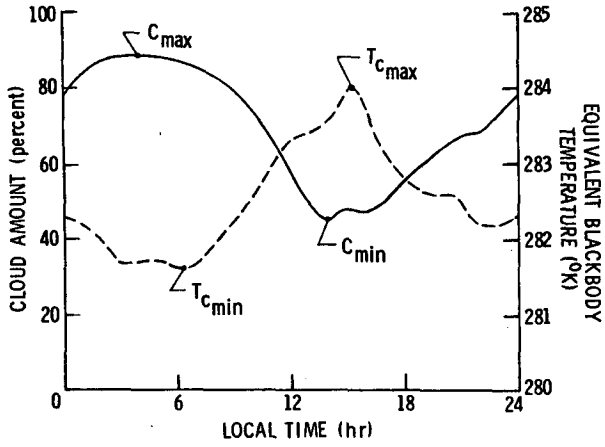

FIG. 8. Mean November 1978 cloud amount and cloud-top temperature for a 250 × 250 km² region at 21.4°S, 86.3°W.

coast from west to east, the cloud cover increases, then decreases in the regions nearest to, but not on, the coast. Coastal cloudiness shows a different behavior: it reaches a minimum value after sunset, then begins to increase until the next morning.

These diurnal changes in cloudiness are easily seen in the GOES photographs on nearly any day during November 1978. Figs. 10 and 11 are GOES-East visible and infrared images, respectively, which include the Pacific stratocumulus (Sc) areas and western South America. These images were recorded on 10 November 1978, at 1400 and 2000 GMT corresponding to 0800 and 1400 LT, respectively, at 90°W. In Fig. 10a, the area west of 90°W is not very well illuminated, but it is light enough to show the heavy cloud cover (>50%) extending diagonally to the northwest from 30°S and 72°W. Six hours later, (Fig. 10b) much of the cloudiness is gone from the area. The thinner parts are almost totally dissipated, while the heavier portions are considerably diminished. Note that the cloud cover in the area near the Peruvian coast between 72 and 77°W appears to have increased.

This change in cloudiness over six hours is also evident in the infrared images. The Sc clouds in Figs. 11a,b are a dull gray shade and have a more continuous character than those seen in Fig. 10. This untextured appearance results from the lower spatial resolution of the infrared imaging system and the coarse gray scale used in this photograph. The effect in the infrared is no less dramatic since the cloud cover over this entire area appears to diminish by a factor of 2 in six hours.

b. Northern South America

The land area north of 20°S in South America includes the Amazon River Basin. The diurnal periodicities in mean total cloudiness over the Amazon are not entirely in phase from region to region although the phases of the diurnal variations in C_1 and C_3 are common to most of the regions (Fig. 3). These common characteristics result from a diurnal cycle in cloudiness typified by the results shown in Fig. 12a for a region centered at 5.6°S, 61.9°W. Low cloud cover appears to increase gradually in the morning hours reaching a maximum near noon. Midlevel clouds build steadily in the evening hours

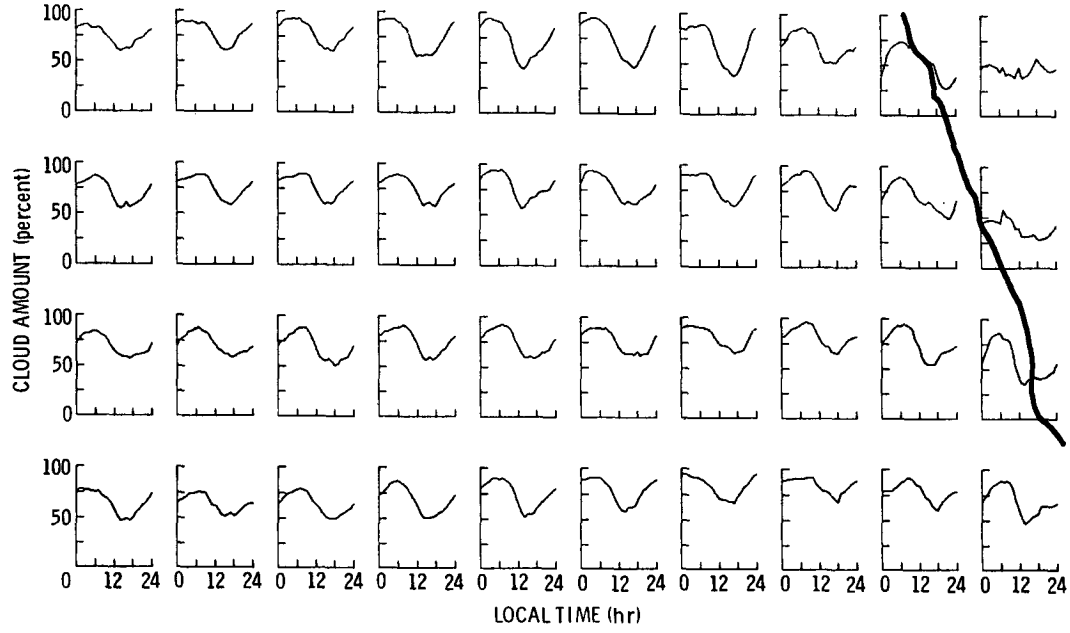

FIG. 9. Mean November 1978 cloud amount for 250 × 250 km² regions between 9 and 18°S, 99 and 76.5°W. Heavy line represents South American coastline.

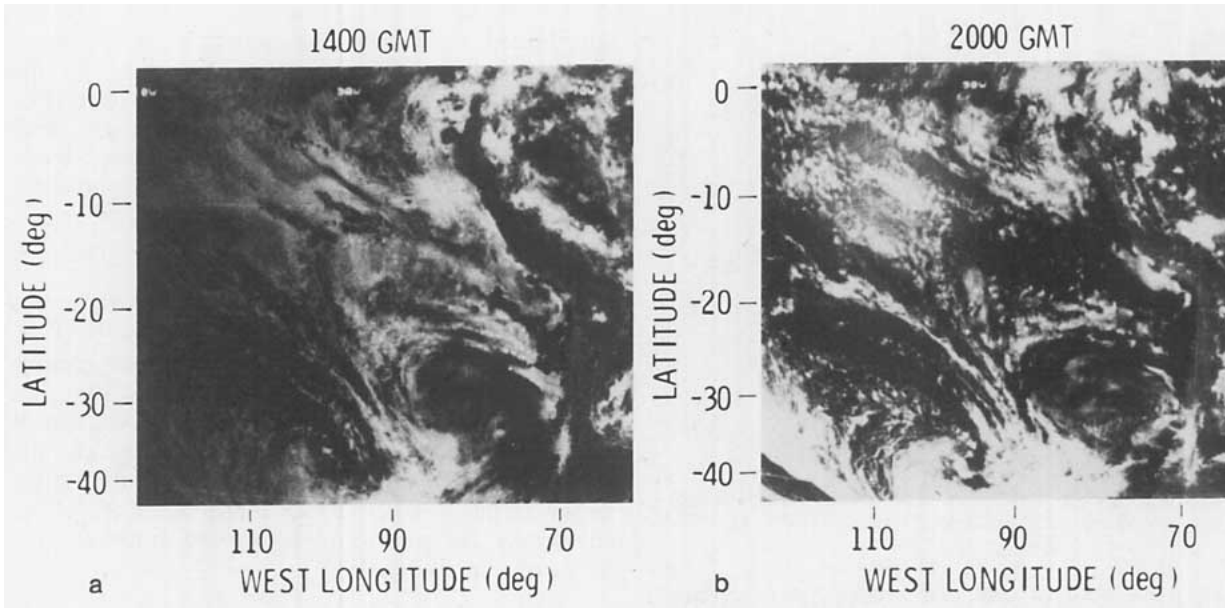

FIG. 10. GOES-East visible images for 10 November 1978.

from a minimum during midafternoon to a peak near sunrise followed by a steady decrease throughout the sunlit portion of the day. The areal fraction covered by high clouds (probably tops of cumulonimbus and associated cirrus) increases rapidly in the afternoon to a maximum near sunset. The middle-level cloudiness may be comprised of thin cirrus outflow from the deep convection associated with the afternoon development of high clouds in addition to altocumulus and vertically-developed cumulus clouds. Some of the afternoon midlevel and evening low-level clouds may be obscured by the high clouds. The early-morning trend found for the low clouds may be the result of low-level fog or stratocumulus forming during the night and being revealed to the satellite as the higher clouds dissipate. Examination of GOES visible imagery reveals that, generally, the low clouds seen later in the morning hours are developing "popcorn" cumuli which give rise to afternoon cumulonimbus cells. These images also reveal an organizational change during midday which is characterized by many small, bright cells in the late morning

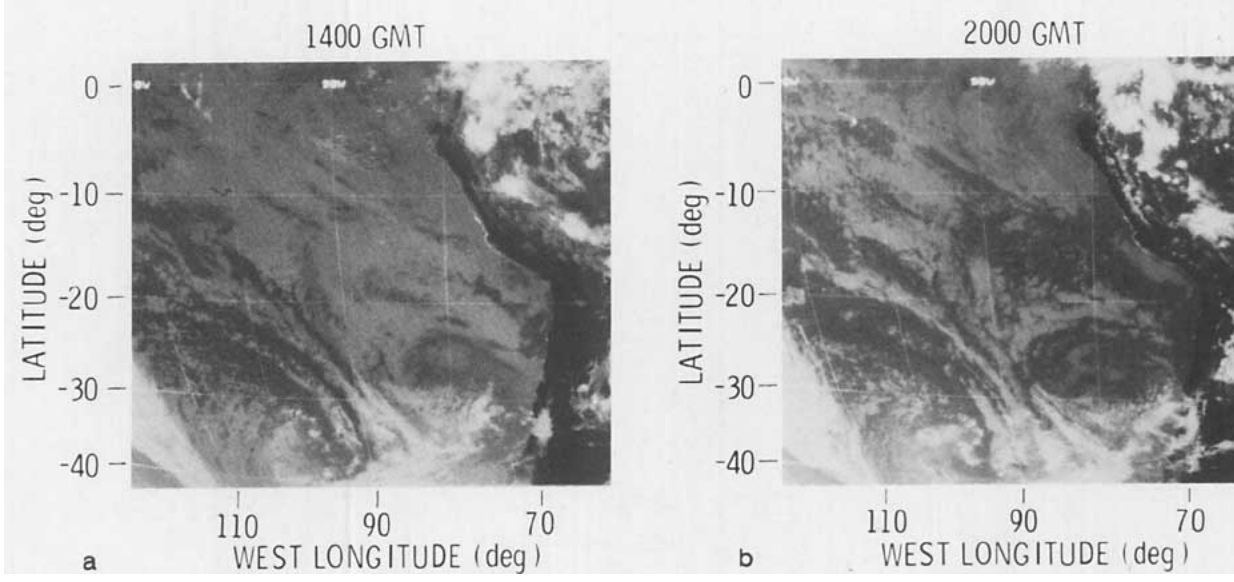

FIG. 11. As in Fig. 10 but for infrared images.

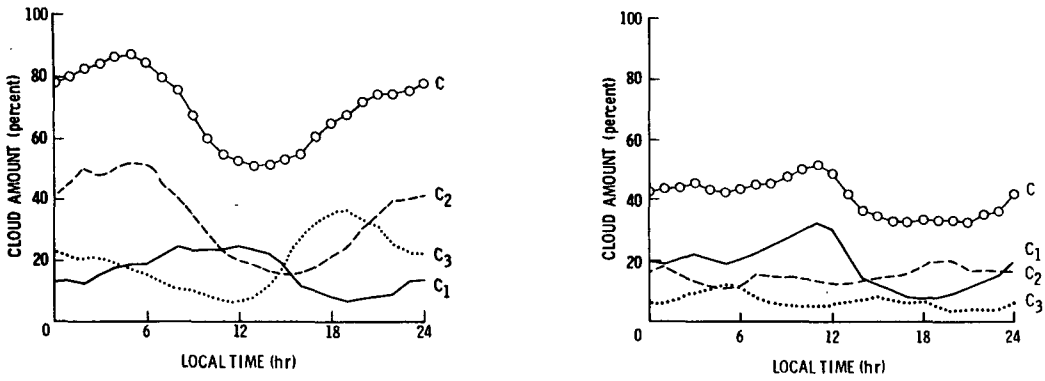

FIG. 12. Diurnal variation of total, low, middle and high cloud cover for November 1978.

followed by a few large cells with extensive cloud-free areas between them. This organization is usually short-lived as the cells mature and develop sizable cirrus shields.

Deep convective activity appears to diminish toward the Atlantic coast as indicated by the decrease in ΔT_c seen in Fig. 5. Cloud data for a region at 5.6°S and 43.9°W are shown in Fig. 12b. Here, the variations in low clouds are similar to those in Fig. 12a, while the diurnal changes in C_2 and C_3 are considerably different. Low cloudiness is the most abundant type and dominates the diurnal cloud cycle. Thus, maximum cloud cover occurs before noon. The familiar "popcorn" cumuli build up rapidly in the morning, but seldom develop into deeper cloud systems. This is also evident in Fig. 4 where $\bar{T}_c$ decreases from the midcontinent to the Atlantic coast. The C_3 maximum which occurs before sunrise in this region is not a common feature of the larger area. This region is one of the few where the C_3 semidiurnal component is greater than the diurnal component. The late afternoon maximum in C_3 usually found elsewhere over the Amazon Basin seems to have been replaced by $C_{2\max}$ in the early evening over this region. Over the Atlantic coastal areas, cumulus growth appears to begin earlier (C_1 peaks near 0900 LT, see Fig. 3b) and shows less vertical development than that seen farther inland (see Figs. 1c and 1d).

Another view of the coherent diurnal periodicity in convection over the Amazon Basin is illustrated in Fig. 13. This figure shows C_3 at four times, six hours apart for every other 250 × 250 km^2 region in South America at latitude 5.6°S. Time is given in GMT and in LT based on the center longitude in the figure. The value of C_3 is assumed to be a good indicator of the intensity of convection. Maximum values of C_3 occur between 1400 and 2000 LT over all of the regions, except at 43.9°W (Fig. 12b). The averages of C_3 for all 11 regions range from 0.13 at 2000 LT to 0.07, the minimum, at 0800 LT.

c. *Southern South America*

There are also many regions in South America poleward of 20°S with significant diurnal variations in mean total cloudiness. Diurnal changes in regional cloudiness over the entire area are not in phase but show some consistent features. An examination of Fig. 3 reveals a pattern of $t_{3\max}$ values which are roughly the same along constant meridians between latitudes 22 and 35°S. To further distinguish this longitudinal structure, C_3 is plotted in Fig. 14b for each region from the Andes to the eastern edge of the grid at latitude 25.9°S in the same manner as in Fig. 13. A crude profile of elevation is shown in Fig. 14a. These data show an apparent eastward propagation of a high cloud maximum. This "diurnal

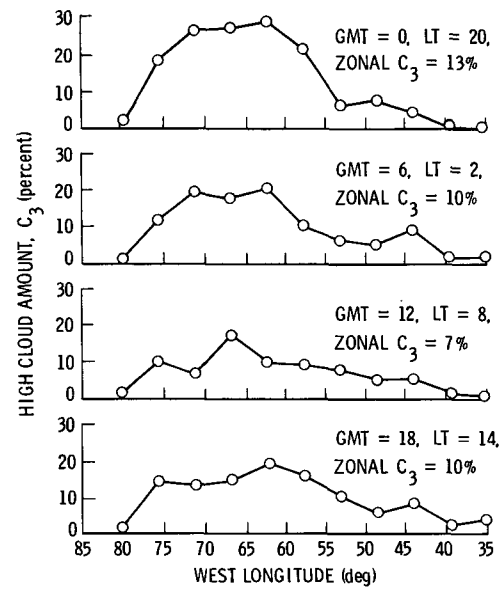

FIG. 13. As in Fig. 12 but of mean high-cloud cover over South America at 5.6°S.

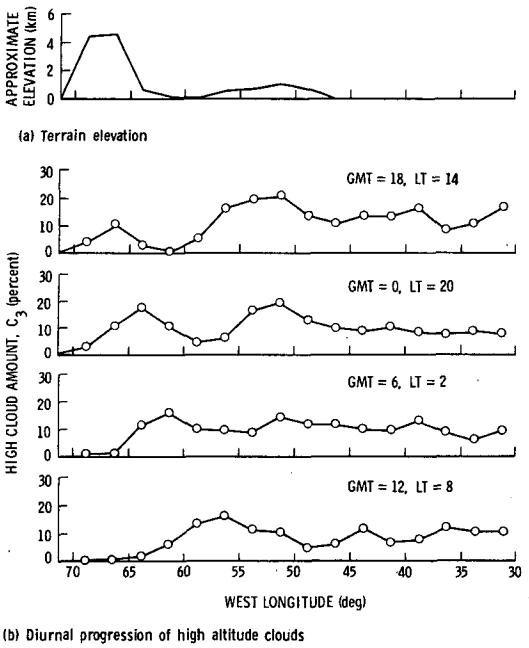

FIG. 14. As in Fig. 12 but of high-altitude clouds over South America at 25.9°S.

wave" appears to originate in the Andes at 66.3°W during the afternoon and progress onto the plains after midnight. This relative maximum appears to dissipate after passing over the Brazilian Highlands, although some minor peaks suggest its continuation well into the Atlantic. This diurnal progression of maximum high cloudiness across meridians is found at each latitude through 37°S, but the passage of the wave over the Atlantic becomes less apparent farther south. Also, the most intense convective activity (highest C_3) at each latitude occurs in regions inland from the Atlantic coast.

South of 37°S, the land mass narrows considerably and is more subject to the influence of cyclonic storms. Vertical changes in cloud distributions follow the same course of events mentioned earlier, but seem to be less pronounced. There is still some evidence of a propagating "diurnal wave." At these latitudes, it appears to come in from the Pacific at a low amplitude, cross the Andes and intensify over Patagonia.

d. Intertropical convergence zone

The ITCZ includes three large areas of intense convective activity ($\bar{C}_3 > 0.10$) separated from each other by broad expanses of relatively suppressed convection covering about 40° of longitude. The most active areas at 10.1°N are indicated by the peaks in $\bar{C}_3$ shown in the bottom half of Fig. 15. The top half of Fig. 15 shows the values of $t_{3\max}$ for 10.1°N. This time varies from region to region with maximum high cloudiness occurring around 1500 LT over a majority of regions and in the morning hours before sunrise over a few regions. The average values of C_3 for the entire zone range from 0.10 at 1100 LT to 0.12 at 1800 LT, a normalized range of 0.20. The diurnal ranges in total and stratified cloudiness over the ITCZ are not as dramatic as those found over the previously discussed areas, but in some cases are statistically significant and highly varied. Fig. 16 shows the diurnal variations in cloudiness over four regions along latitude 10.1°N. This figure illustrates the diversity of cloud variability found within the ITCZ. Fig. 16a shows a region over the Atlantic at 43.9°W, one of the areas of heaviest cloud cover in the ITCZ. The diurnal variability of C is minimal while C_3 varies by 0.08, a normalized range of 0.7. The rather broad maximum in C_3 seen here is found in many of the regions at this latitude. These broad maxima in C_3 are quite distinct from the single, peaked maximum in high cloudiness found over much of the Amazon. Similar differences were found between high clouds in the GATE area (eastern Atlantic) and in South America by Weickmann *et al.* (1977). Two regions of low total cloud cover are shown in Figs. 16b and 16c. In the region over the Pacific at 100.1°W (Fig. 16b), C_3 peaks around

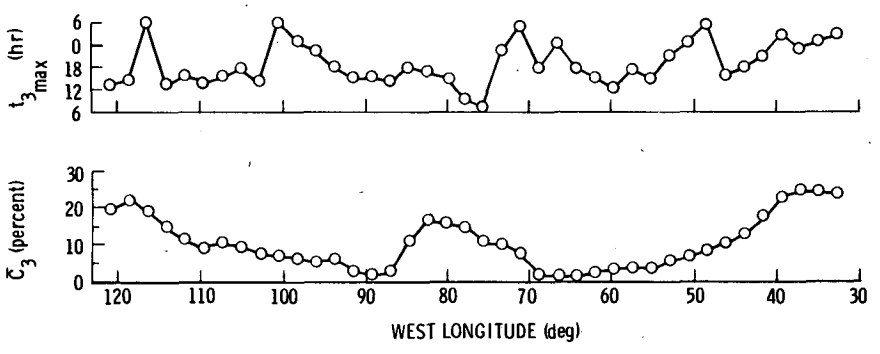

FIG. 15. Average high-cloud fraction at 10.1°N and time of maximum average high-cloud amount for November 1978.

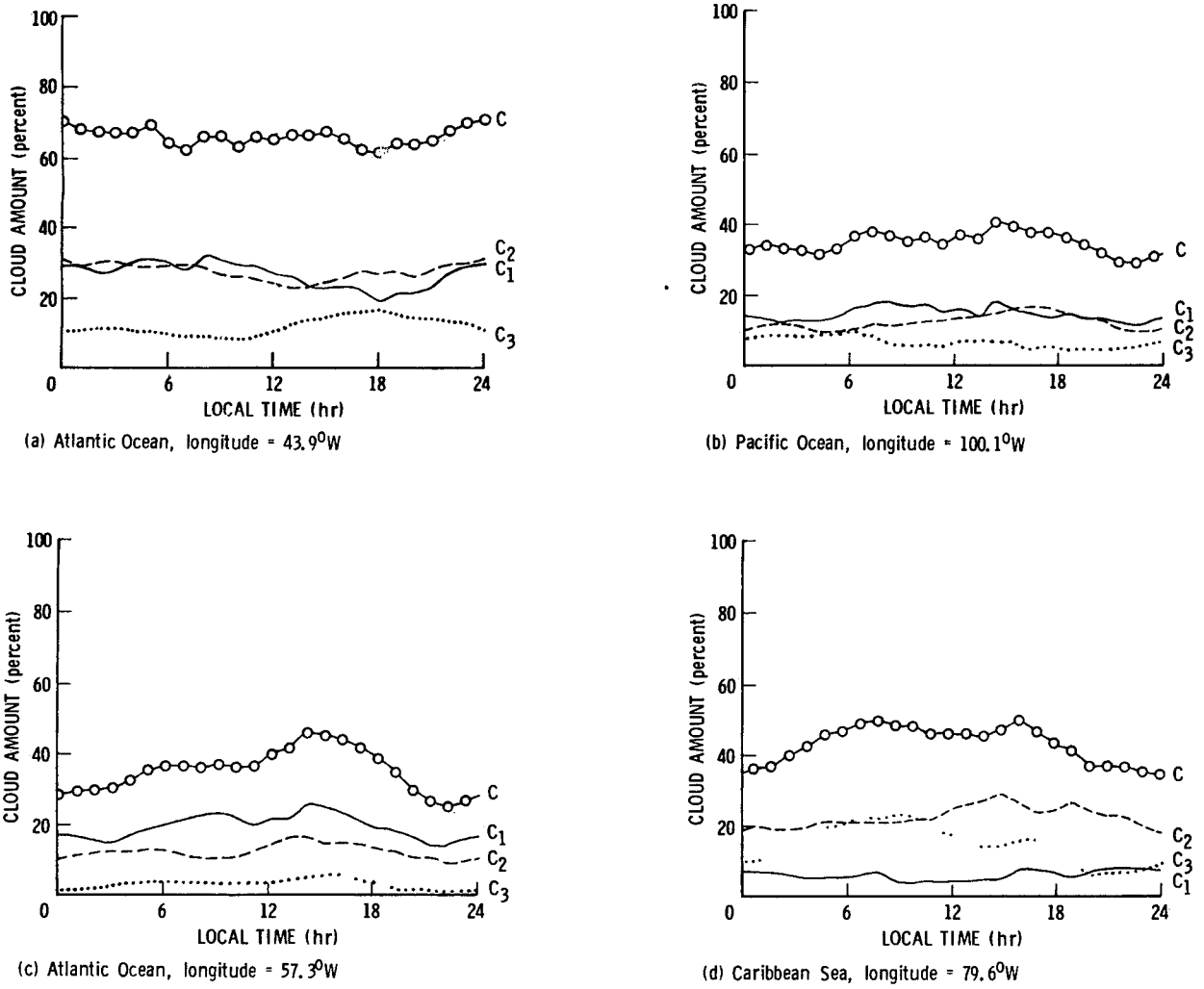

FIG. 16. As in Fig. 12 but of total, low, middle and high cloudiness for regions in the ITCZ at 10.1°N.

sunrise with a minimum after sunset. A slight secondary maximum in C_3 occurs near 1400 LT Over the Atlantic at 57.3°W (Fig. 16c), the high cloud maximum is seen at 1600 LT with a broad minimum centered around midnight. Note the similarities in the shapes of the low and total cloud curves for these two regions. Both show $C_{1\max}$ and $C_{\max}$ occurring at 1400 LT and low and total cloud minima at 2200 LT with similar increases in both quantities until approximately 0900 LT A convectively active, mixed land and ocean area in the Caribbean Sea at 79.6°W (Fig. 16d) shows a primary maximum in C_3 near 0900 LT and a slight secondary maximum during the late afternoon. Minima in middle and high cloudiness are found during the night in this area.

e. Other areas

Diurnal cloud variability is evident in many areas besides those discussed above. The diurnal ranges in these other areas are not as large, $\Delta C < 0.20$, and the phases of the diurnal cloud variations are not as coherent over large spatial scales as they are over regions south of 10°N. Fig. 17 depicts the diurnal variability of cloudiness over four regions north of 10°N. These regions are not necessarily typical of any large areas of the grid; they are shown, primarily, to illustrate the wide variety of cloud behavior found in the northern portion of the study area.

At 23.6°N, 51.3°W (Fig. 17a), low- and middle-level clouds appear to be in phase, with both peaks occurring near noon although the mid-cloud peak is rather broad. These maxima follow the late-morning minimum in C_3. High clouds also show a broad maximum which extends from midafternoon well into the evening. Although Fig. 3 indicates that many areas in the North Atlantic show maximum total cloudiness occurring during midday, the vertical distribution does not always follow the sequence of events seen in Fig. 17a. High- and low-level cloudiness

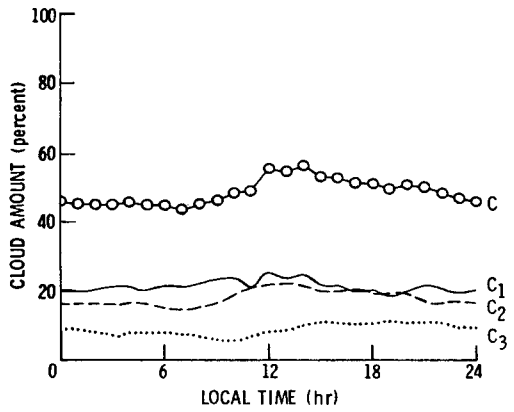

(a) Mid-Atlantic, latitude = 23.6°N, longitude = 51.3°W

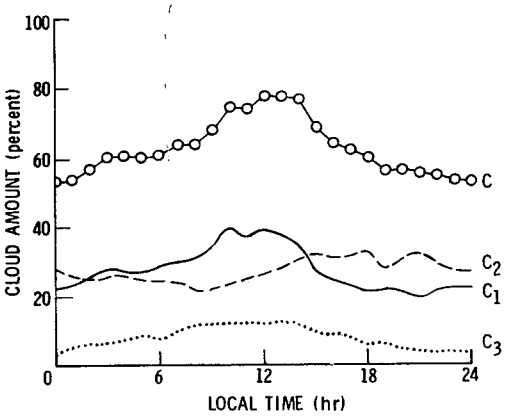

(b) Atlantic Ocean east of U.S., latitude = 32.6°N, longitude = 76.3°W

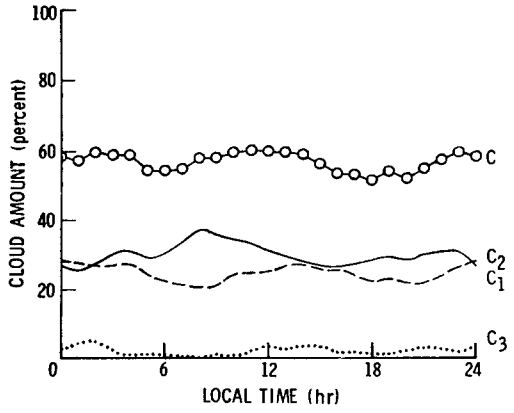

(c) U.S. region, latitude = 39.4°N, longitude = 88.5°W

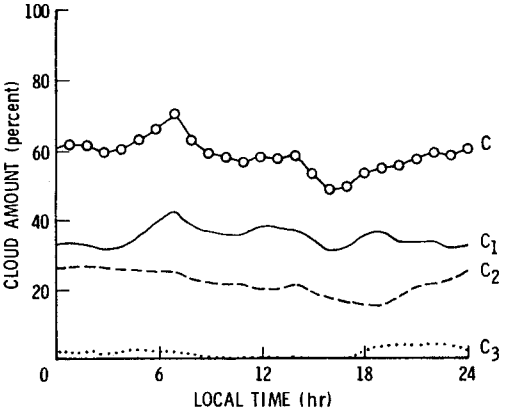

(d) Western U.S. mountains, latitude = 37.1°N, longitude = 106.5W

FIG. 17 As in Fig. 12 but over four regions in the Northern Hemisphere.

seem to be in phase over the region at 32.6°N and 76.3°W shown in Fig. 17b. Cloudiness peaks around noon at both levels, while midlevel clouds seem to have a broad maximum extending from midafternoon well into the night. The diurnal cloud variability over this region is typical of the areas along the southern Atlantic coast of North America.

During November, North America is subject to many traveling synoptic-scale disturbances. Thus, diurnal effects are more likely to be diminished on an average basis. This is apparent in the case of total cloudiness, but even in areas where C is relatively constant, such as the region at 39.4°N and 88.5°W in Fig. 17c, the vertical variation in cloudiness is still quite evident. Low-cloud cover, ranging from 0.25 in midafternoon to 0.37 around 0800 LT, is out of phase with C_2 and C_3 with two minima near 1500 and 0100 LT Middle- and high-level cloudiness appear to be in phase, with two peaks occurring around midnight and shortly after noon. As noted in the previous section, some midlevel cloudiness may actually belong to the high-cloud category

Diurnal cloud variability is generally greater over Mexico and the Rocky Mountains than elsewhere in North America. This should be expected given the effect of mountains on local circulations, though it is not evident that a common cycle exists over the entire area. However, most areas show a relatively sharp increase in mean cloudiness around sunrise as exemplified in Fig. 17d for a mountainous region centered at 37.1°N and 106.5°W Low-cloud cover increases by ~0.10 between 0300 and 0700 LT It reaches a minimum during the late afternoon. Middle and high clouds are most frequent during the night. Most surface observations taken in this region also show similar trends for total cloudiness: a sharp increase around sunrise and a minimum during the late afternoon and early evening. West of California there appears to be an active Sc cycle. Low-cloud cover comprises from 65 to 90% of the total cloud

fraction over the Pacific in this area (Fig. 1); maximum cloudiness occurs around sunrise; and $\Delta C \approx 0.20$. The absolute diurnal ranges in low cloudiness here are not as large as in the Sc area in the southeastern Pacific. Additional data from regions west of those shown in Fig. 1 (out to 138°W) show similar phases and ranges in low and total cloudiness.

4. Discussion

The preceding results have shown that diurnal variability of cloudiness was an important feature over a considerable portion of the Western Hemisphere, especially the tropics, during November 1978. Because of the relatively fine temporal resolution and the large area covered, it has been possible to show several coherent, large-scale diurnal cloud variations as well as a wide variety of regional-scale (250 km) diurnal cloud cycles. In this section, the results will be discussed in light of previous observations of the diurnal behavior of cloudiness. A comprehensive explanation of the cloud phenomena reported above is beyond the scope of this paper. Some of the following discussion, however, will be devoted to the physical mechanisms which may be responsible for the observed diurnal cloud variability.

a. Land areas

The late afternoon–early evening maxima in high cloudiness over tropical South America and Central America are consistent with the observations over other tropical land areas (e.g., Reed and Jaffe, 1981 and Short and Wallace, 1980). Jaffe (1982) found a pronounced late afternoon–evening maximum in high cloudiness over much of tropical Africa which is quite similar to the present results for most of the Amazon Basin. Deviations from the usual late afternoon $C_{3\max}$ may be attributed to localized mountain–valley or land–sea breeze circulations. For instance, $C_{3\max}$ occurs near 0300 LT over several regions in northeastern Brazil in the vicinity of 5°S and 40°W (e.g., Fig. 12b). These exceptions to the general trend correspond to the nocturnal (2100 to 0900 LT) maxima in rainfall reported by Kousky (1980) who deduced that the phases of the rainfall maxima in these low-lying regions result from mountain-valley circulations. Another example of the influence of local geography on the diurnal cloud cycle is shown in Fig. 18 for a region at 10.1°N, 71.8°W in Venezuela. The two relative maxima in late afternoon and early morning probably result from a strong sea–land breeze between the Lago de Maracaibo and the mountainous regions to its east. It is also likely that the morning $C_{3\max}$ found over other regions in Panama and Colombia is due to complex circulation patterns resulting from the intricate terrain and coastlines in that area.

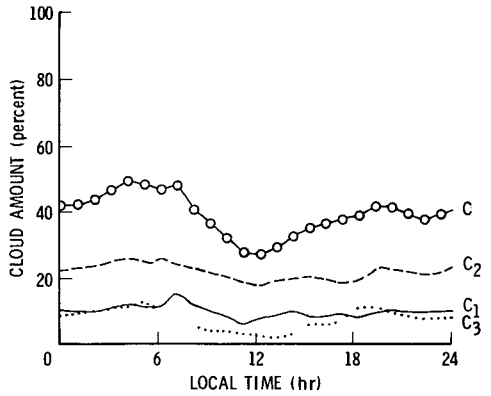

FIG. 18. Example of November 1978 diurnal cloud variations over a region at 10.1°N, 71.8°W containing mountains and lowlands.

The common development of afternoon thunderstorms over the remainder of northern South America is probably the result of destabilization of the boundary layer by surface heating in the morning accentuated by slight variations in local topography This terrain effect is suggested by the occurrence of low-cloud patterns which outline the major rivers (e.g., the Amazon and Orinoco) and their largest tributaries. These patterns are frequently evident in the GOES visible imagery at 1600 GMT, which is $t_{1\max}$ in many regions. The remarkably coherent pattern in $t_{3\max}$ and the magnitudes of ΔC_3 suggest that a continental-scale, diurnal circulation feature exists between the Amazon Basin and the surrounding areas. From the average November and February upper-wind data of Sadler (1975), the analysis of the February 1975 tropospheric circulations over South America (Virji, 1981) and the relative magnitudes of $\bar{C}_3$ in Fig. 1d, it may be concluded that, on the average, net divergence occurs at the upper levels and net convergence at the lower levels of the atmosphere over most of the Amazon Basin during November. If it is assumed that the value of C_3 is directly proportional to the rate of ascending air, then it follows that the upper-level divergence over most of the Amazon undergoes a diurnal cycle which is not entirely compensated locally Thus, the subsidence rate over adjacent areas must have a diurnal variation to balance the diurnal cycle of divergence over the Amazon Basin. This implies the existence of a diurnal circulation system akin to a large-scale sea–land breeze. Further development of this picture of the Amazon area as a diurnally pulsating, large-scale source of upper-level air is given later in this paper.

The pattern of daytime $C_{3\max}$ over the Andes south of 20°S and the nocturnal $C_{3\max}$ over the adjacent lowlands (see Figs. 3d and 14) is much like the distribution of summertime thunderstorm frequencies over the United States reported by Wallace (1975). His results show a maximum frequency of thunder-

storms in the afternoon over the Rocky Mountains and near midnight over the Great Plains. Phillip (1979) examined the convective interactions over that same area in detail and concluded that the observed diurnal behavior resulted from a mountain–plains circulation. An Andes–Gran Chaco and a Gran Chaco–Highlands–Atlantic coast circulation system with rising air over the Andes and Brazilian Highlands and descending air over the Gran Chaco and Atlantic coast during the afternoon and sinking air over the mountains and rising air over the lowlands during the late night–early morning period may account for the observed diurnal variations in C_3 over this area. Further discussion of the factors controlling such circulation systems can be found in a numerical model study by Paegle and McLawhorn (1983).

The occurrence of maximum mean middle cloudiness during the late evening (Fig. 3c) over many land areas was also found by Short and Wallace (1980). There are, however, at least as many areas in Fig. 3c with C_{2max} between midnight and 0600 LT as there are in the evening in the present case. Minimum middle cloudiness was found most often between 0800 and 1200 LT indicating that measurements of C_2 taken at any time besides late morning would be greater than that in the morning. Thus, measurements of C_2 taken at 0900 and 2100 LT would almost always yield an evening bias in midlevel cloudiness.

The morning maxima in low clouds over most of North America are probably tied to the generally stable stratification of the lower atmosphere during November. Thus, St and Sc clouds occur much more frequently than cumulus (e.g., Haragan, 1969). Solar heating of the surface and boundary layer during the morning would tend to dissipate low-level boundary layer clouds through turbulent mixing and warming by sensible heat transfer. The midday maxima in C_1 over the tropical land areas result from the surface warming of the convectively unstable lower atmosphere in the tropics during the morning followed by the dissipation of many low clouds at the expense of developing cumulonimbus cells.

b. Oceans

While there are few oceanic regions where the diurnal variations in C_3 were considered statistically significant, it is significant that C_{3max} (Fig. 19a) occurred in the afternoon over more than 60% of all considered ocean regions. (If a uniform distribution is assumed for the number of regions with a given t_{3max}, then it may be concluded at a confidence level greater than 0.99 that the present results do not come from a uniform distribution.) The afternoon maxima in high cloudiness observed over the GATE area (e.g., Gruber, 1976; Ball *et al.*, 1980) and the present results appear to be at odds with the more global conclusions reached in a number of earlier investigations. For

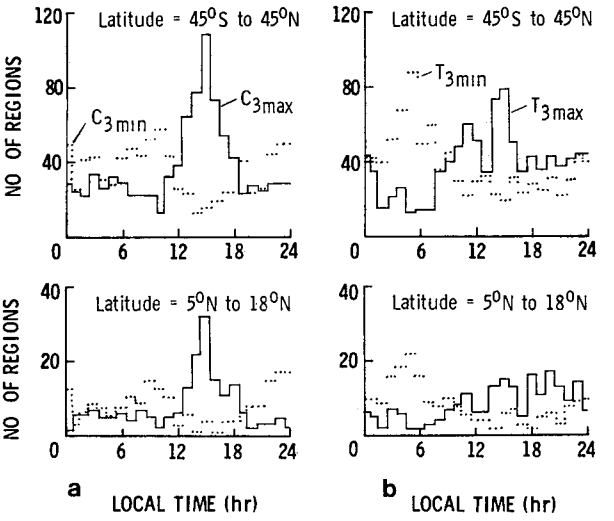

FIG. 19. Time of occurrence of maximum and minimum (a) high-cloud amounts and (b) high-cloud-top temperature over ocean regions during November 1978.

example, Short and Wallace (1980) inferred a widespread morning bias in the frequency of thick, high cloudiness over low-latitude oceans which is consistent with the existence of an early morning maximum in heavy precipitation proposed by Gray and Jacobson (1977). The discrepancies between the previous and present observations may be due to differences in temporal and spatial sampling and in the actual measured quantities. Short and Wallace (1980) reached their conclusions based on the doubling of the frequency of occurrence of IR temperatures < 223 K from 2100 to 0900 LT over the Pacific Ocean between 20°N and 20°S during the summer months. The present definition of high clouds varies with region (see Minnis and Harrison, 1984a), but generally includes IR temperatures < 250 K, with average high-cloud temperatures around 230 K. If the differences in the observations are due only to the frequency of the *highest* clouds, then T_3 in the morning hours should be lower for a widespread morning maximum in the highest convective clouds. This appears to be the case for the ITCZ by itself and for all ocean regions in the study area as shown in Fig. 19b. Minimum T_3 and C_3 were found most frequently around 0500 LT, while T_{3max} occurred most frequently around 1500 LT over all ocean regions together and during the afternoon and evening over the ITCZ regions. A similar result can be derived from Figs. 3d and 3e of Short and Wallace (1980) if the total number of pixels < 253 K is considered. This out-of-phase relationship between high-cloud temperature and high cloud cover is in contrast to the nearly coincident values of T_{3min} and C_{3max} found over the Amazon Basin.

Threshold IR temperatures associated with precip-

itating convective clouds range from 253 (Griffith *et al.*, 1978) to 235 K (Arkin, 1979). Therefore, high clouds as defined by Short and Wallace (1980) and in the present study are highly correlated with precipitation. If cloud-top temperature is inversely proportional to the rainfall rate, then the present results are also consistent with the conclusions of Gray and Jacobson (1977) that the heaviest rainfall occurs in the morning over tropical areas. Precipitation would be most widespread, however, during the afternoon and would occur at a lower rate.

The high interregional variability in t_{3max} (Fig. 3d) suggests that the development of high clouds over a given marine area is a very complex process which is regionally dependent to some extent. Nonetheless, it seems that some global-scale mechanism is required to explain the tendencies for afternoon high-cloud maxima and morning high cloud-top temperature minima. One possible explanation for the afternoon maxima is the existence of a hemispheric tropospheric tidal circulation driven by the mean net daytime-minus-nighttime tropospheric temperature differences as proposed by Foltz and Gray (1979). The 1500 LT maximum in C_{3max} corresponds to the time of maximum upward vertical velocity above the boundary layer in their idealized model of this diurnal solar tide. Gray and Jacobson (1977) have argued that the morning enhancement of deep convection over the tropical oceans is due to the differences in tropospheric radiative cooling between cloudy and cloud-free areas. This mechanism may be responsible for the observed maximum frequency of T_{3min} in the early morning. Another mechanism, proposed by Brier and Simpson (1969) to explain the diurnal cycle in cloudiness and precipitation in the tropics, is the semidiurnal pressure wave forced by heating of ozone in the upper stratosphere. While the exact mechanism relating the S_2 pressure wave and weather is still not understood, the empirical results of the Brier and Simpson (1969) study indicate that the S_2 effect tends to "enhance cloudiness and precipitation around sunrise and sunset and to suppress them near midday and midnight." Results of the harmonic analysis of C_3 (Fig. 7) show the prevalence of a weak S_2 component centered around 0300 LT, about 3 hours earlier than that found by Brier and Simpson (1969), but consistent with the proposed S_1 tide. The diurnal component of $C_3(t)$ in Fig. 7a, however, shows no strong tendency to maximize at 1500 LT. The frequency distribution of the phase of $S_1(C_3)$ is somewhat more uniform than that of C_{3max}, but skewed toward the afternoon with a peak near 1700 LT. Thus, it is not obvious which, if any, of these mechanisms is primarily responsible for the observed behavior of C_3.

The middle cloud maxima over the oceans were found most often (43% of all regions) between 1800 LT and midnight. Another 27% of the regions had C_{2max} occurring between midnight and 0600 LT, while C_{2min} was found between 0600 LT and noon over 43% of the marine regions. These results are essentially in agreement with the widespread evening bias in midlevel clouds deduced by Short and Wallace (1980). The temporal sampling limitations in their data set precluded the detection of a middle cloud bias between 0000 and 0600 LT. The reasons for the prevalent nocturnal maxima in C_2 over both land and ocean are also not entirely clear at present, although over convectively active land areas, the nocturnal decay of solar-induced deep convection (evident in the magnitude of C_3) would probably produce convective cloud tops which gradually decrease in altitude (evident as middle clouds). As static stability returns to these regions during the night, stratiform clouds may form within the middle troposphere from the residual moisture introduced from below by the earlier convection.

The frequent occurrence of maximum mean low cloudiness near sunrise over marine areas (54% of all ocean regions) is consistent with the conclusions of Short and Wallace (1980) that a morning bias in low clouds is a widespread phenomenon over low-latitude oceans. That conclusion may be extended to include the midlatitude oceans as well, since the frequency distributions of t_{1max} (not shown) poleward of 30° latitude are nearly identical to those regions on the equatorial side of 30° latitude. The occurrence of a midday C_{1max} over a significant number (27%) of regions, however, would have been missed in the Short and Wallace (1980) data set since C_{1min} is found most often during the afternoon and evening over the oceans. Therefore, measurements taken at 0900 and 2100 LT would almost always yield a morning bias in low cloudiness. Other evidence of afternoon maxima in maritime low cloudiness was reported by Ball *et al.* (1980). They found low cloud maxima near 0400 and 1500 LT over the GATE area (~8°N and 20°W). Similar double maxima were found in the present data set over the Atlantic near the equator where the phases of $S_2(C_1)$ are 0300 and 1500 LT (Fig. 6b). Holle and MacKay (1975) observed an early morning low-cloud maximum over the Atlantic near 13.1°N and 59.5°W during the summer. An 0400 LT C_{1max} was found in the present study for many of the regions in that same locale, indicating little seasonal dependence of the diurnal variations in low cloudiness in that part of the Atlantic. The above examples of t_{1max} from ship observations over the Atlantic indicate that some variation in t_{1max} should be expected from the satellite-based observations. It should also be noted that the exact time of C_{1max} is not completely certain in those areas where $\bar{C}_2$ and $\bar{C}_3$ comprise a significant portion of the total cloud amount since low clouds directly underneath higher clouds will not be detected. Over much of the Pacific, where low clouds are the primary cloud type, the value of t_{1max} is more certain. The morning low-

cloud maxima seen over the Pacific west of California (Fig. 3b) were also observed by Simon (1977) during several other months of the year, suggesting that the phase of $C_{1\max}$ is seasonally independent over that area. The patterns of statistically significant morning-to-evening differences in outgoing IR over the southeastern Pacific given by Short and Wallace (1980) are quite similar to the unshaded southeastern Pacific areas in Fig. 3b, again indicating a seasonal consistency in $t_{1\max}$ over those regions.

c. *Marine stratocumulus and large-scale divergence*

Given the climatological similarity of the southeastern Pacific to other large oceanic regions (Agee *et al.*, 1973; Schubert *et al.*, 1979) and the role of marine stratocumulus in the global circulation, it is important to understand the causes of the pronounced diurnal cloud variability observed over this large area. A number of researchers (e.g., Schubert, 1976; Albrecht, 1981; Fravalo *et al.*, 1981) have developed marine boundary layer cloud models which indicate that a radiative mechanism can drive diurnal cloud cycles over the open ocean. Hanson and Gruber (1982) demonstrated that the diurnal solar cycle can force a thinning and lowering of the cloud layer during the day with minima in cloud thickness and height occurring in the midafternoon and cloud height and thickness maxima near sunrise. The thinning of the cloud layer is somewhat equivalent to the decrease in cloudiness observed over the southeastern Pacific. It may also explain the large diurnal variations in cloud albedo over that area (Minnis and Harrison, 1984b). The decrease in cloud-top altitude corresponds to an increase in T_c as seen in Fig. 8. Brill and Albrecht (1982) concluded that the solar cycle is the primary source of the diurnal variations in the trade Cu field driving a cloud cycle with peak cloudiness near 0800 LT and a minimum in the late afternoon. They showed that divergence had a minimal effect on the phase, but increased or decreased the amplitude of the cloud cycle depending on the phase of the divergence. Their study, however, considered relatively low-amplitude variations in the divergence field. An increase in the divergence variation would be likely to enhance the relative effect of large-scale divergence on the diurnal oscillations of cloudiness. Roach *et al.* (1982) have also concluded that the subsidence rate is an important control in mesoscale Sc variations.

During the spring months, there are large differences in the ranges of the diurnal variations of low clouds over the northeastern Pacific ($\sim$0.13 according to Simon, 1977) and the SEP (up to 0.45 in the present study). Geographical variations in the diurnal cycle of large-scale divergence may help explain these differences. From Fig. 2 of Short and Wallace (1980), it appears that the only other area which may have a diurnal variation in low clouds comparable to that observed over the SEP is the southeastern Atlantic near the southwestern and central African coasts. The other major areas of marine stratocumulus show indications of diurnal variability in low-cloud cover (Short and Wallace, 1980), but the areal extent and magnitudes of these indicators are much less than those over the southeastern Atlantic and Pacific Oceans. Is it only coincidental that those last two areas are both adjacent to large rain forests which have coherent, continental-scale diurnal variations in deep convection?

If there are differences in the diurnal cycles of large-scale divergence over the various eastern oceans, perhaps they are the result of differences in the convective processes occurring over adjacent land masses. In Section 4a, it was concluded that the doubling of high-cloud cover from morning to evening over the Amazon Basin indicates a significant diurnal pulse in the large-scale divergence field. Over the western half of the United States, there is also a widespread afternoon maximum in summertime thunderstorm frequency (Wallace, 1975), suggesting an afternoon bias in mass convergence. From climatological differences, it may be assumed, though, that the magnitude of diurnal variations of divergence over North America is much less than that over the Amazon. The manner in which these divergence variations affect the cloudiness over the adjacent ocean cannot be quantified from the present data, but a theoretical discussion of the South American case may be instructive. Compensation for the afternoon increase in rising motion over tropical South America must occur as an increase in sinking motion over some other large areas: in the present case, northeastern Brazil and the SEP. This would suggest a diurnal variation in circulation between the continent and surrounding oceans similar to that proposed by Foltz and Gray (1979). Although the Andes Cordillera prevents exchange of low-level air, there is a possibility of a one-way flow or effect from the Amazon to the Pacific at the upper levels. Howell (1952) observed that the daily convective cycles over western Peru and the adjacent Pacific are directly tied to the convective activity which begins on the eastern slopes of the Andes. Perhaps there is a larger-scale connection between the atmosphere on either side of the Andes.

To examine this possibility, the normalized low-cloud fractions west of 81.5°W and the normalized high cloudiness east of 81.5°W at 5.6°S were plotted for every 4 hours (Fig. 20). It is clear from Fig. 20 that the increase in C_3 over most of South America is nearly simultaneous with a decrease in cloudiness over the SEP. A correlation coefficient of -0.8 was found between C over nine regions west of 81.5°W and C_3 over the nine regions east of 81.5°W at 5.6°S. On the right side of the figure, it is evident that the high clouds east of 50°W are out of phase with C_3

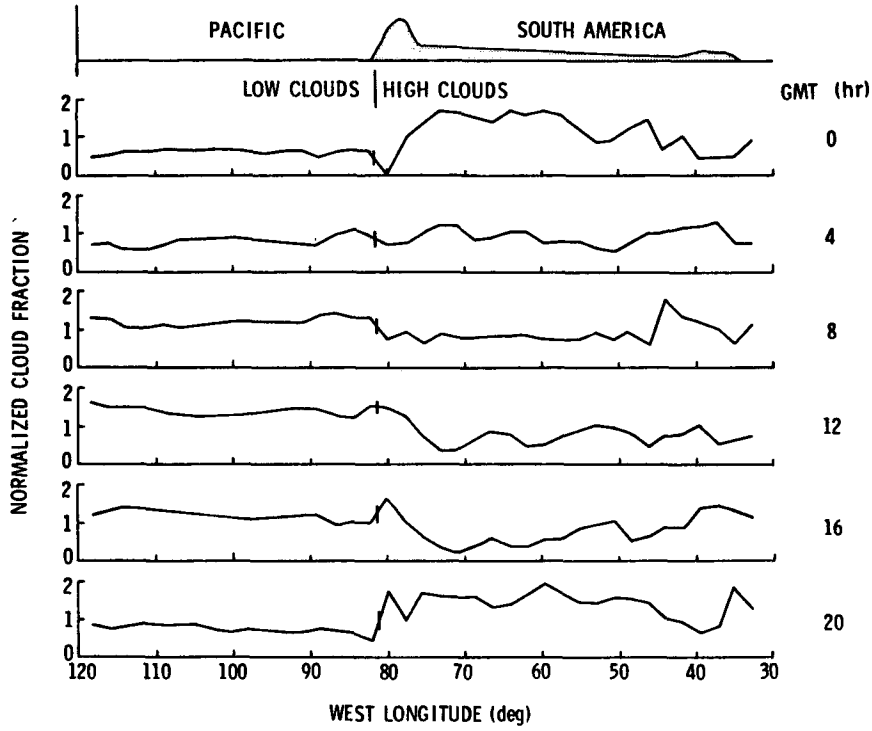

FIG. 20. Diurnal variation of normalized low cloudiness west of South America and normalized high cloudiness over South America at 5.6°N during November 1978.

west of 50°W. While the above out-of-phase relationships may only be coincidental (i.e., any two quantities with a 24-hour periodicity will usually be well correlated at some lag time), the simultaneous occurrence of C_{min} over the SEP, C_{3min} near the Atlantic and C_{3max} over the Amazon strongly suggests some physical relationship.

The wave-like structure in the curves in Fig. 20 indicates that a simple model of a continental-scale, diurnally-dependent circulation is not sufficient to explain the details of the cloud behavior in this area; it is one possible explanation for the largest features. The radiation mechanisms discussed earlier may dominate the Sc diurnal cycle, dictating its phase, while the diurnal variations in divergence forced by convection over the Amazon Basin may account for its large amplitude. Determination of the exact mechanisms that propagate the effects of the variations in the divergence field requires further investigation.

5. Conclusions

The average November 1978 diurnal variability of cloud cover has been documented for the area between 45°N and 45°S and 30 and 125°W. It was found that in all regions there is some response of the atmosphere to the 24-hour solar cycle manifest in diurnal variations in cloudiness which show varying degrees of regularity. The response to the hourly changes in the incoming solar radiation takes the form of changes in the horizontal and/or vertical extent of the cloud cover. Even in the middle latitudes where cyclonic storm passages are frequent, these diurnal variations are still detectable. Diurnal variability in tropical and subtropical areas is much more pronounced.

In general, there are tendencies for clouds to form at a particular altitude at certain local times. Over marine areas, thick high clouds are most frequent in the afternoon, but the lowest cloud-top temperatures (highest clouds) are most common around 0300 LT. Afternoon and evening maxima in high cloudiness occur over most land areas. Middle-level or thin, high cloudiness is most widespread just before sunrise over land and just after sunset over water, regardless of latitude. Low clouds are found most often in the early morning over ocean areas, during midday over tropical land regions and in the morning over mid-latitude land areas. Diurnal variations in total cloudiness are most substantial over regions where clouds predominantly occur at one level in the atmosphere, such as the low cloudiness over much of the southeastern Pacific. Over other areas, the variations of clouds at different levels tend to cancel each other.

The results of this study have shown some general trends, confirmed certain earlier observations and revealed several new aspects of diurnal cloud variability. The temporal and spatial resolution available

in the present data set has permitted the determination of several regional cloudiness characteristics (e.g., times of maximum and minimum cloud cover; and concurrent cloud fraction at three levels over many 250×250 km^2 regions) which were not obtained in a number of earlier studies which utilized other data sets. From the results of this study, it may be concluded that monitoring of the diurnal variability of regional cloudiness requires data taken at a resolution better than every 12 h. Definition of the optimum temporal resolution, however, requires further examination.

The diurnal variations of cloudiness are highly dependent on spatial scale. A wide variety of regional diurnal cloud cycles has been presented that supports the conclusion of Ball *et al.* (1980) that diurnal cloud variations are regionally dependent. At the same time, there is considerable evidence given here that showed that monthly averaged diurnal cloud variations occur at spatial scales ranging from the subregional (<250 km) to continental and, possibly, hemispheric. For example, land–sea breezes within a region may yield double maxima in high cloudiness; continent–ocean differences may lead to diurnal cloud variations coherent on scales up to 3000 km. A global-scale tidal mechanism may help explain the predominant occurrence of high clouds over the ocean during the afternoon. Defining the mechanisms driving these cloud variations and understanding the interaction of these mechanisms at different scales are important topics for future research.

The effects of diurnal cloud variability should be taken into account in models that predict weather and climate, since the diurnal cloud variations are observed at both small and large spatial scales and over time periods up to one month or greater. Interaction of the cloud field with thermodynamic and radiative energetic processes in the atmosphere will depend on the time of day. The large diurnal ranges in total cloud amount and cloud-top temperature also have important implications for the measurement and interpretation of Earth's radiation budget both at the top and at the base of the atmosphere. Large diurnal variations in mean total cloud fraction will probably cause significant diurnal biases in the amount of absorbed and reflected solar radiation in a given region. Substantial diurnal biases in emitted longwave radiation may result whenever the cloud-top temperature undergoes a large diurnal variation. Again, these potential biases in the radiation field may occur at many different spatial scales.

The data used in this investigation represent only a small portion of the globe and the annual cycle. The short averaging period limits the statistical reliability of the results. Because it is a climatological feature, diurnal cloud variability is a function of geography and season. Therefore, any comprehensive understanding of this aspect of clouds will require much additional research utilizing other observations covering more areas and time periods.

Acknowledgments. We would like to thank Messrs. G. G. Gibson, F. M. Denn and J. L. Robbins of Kentron International, Inc. for their assistance in preparing the graphics and in the editing of this paper. Ms. J. Cridlin of the NASA Langley Research Center is gratefully acknowledged for her efforts in typing the manuscript. The computer programming support of Ms. G. Lobo of Computer Sciences Corporation is also appreciated.

REFERENCES

Ackerman, S. A., and S. K. Cox, 1981: GATE Phase III mean synoptic-scale radiative convergence profiles. *Mon. Wea. Rev.*, **109**, 371–383.

Agee, E. M., T. S. Chen and K. E. Dowell, 1973: A review of mesoscale cellular convection. *Bull. Amer. Meteor. Soc.*, **54**, 1004–1012.

Albrecht, B. A., 1981: Parameterization of trade-cumulus cloud amounts. *J. Atmos. Sci.*, **38**, 97–105.

Arakawa, A., 1975: Modeling clouds and cloud processes for use in climate models. *The Physical Basis of Climate and Climate Modeling*, Appendix 4, GARP Publ. No. 16, 183–197.

Arkin, P. A., 1979: The relationship between fractional coverage of high cloud and rainfall accumulations during GATE over the B-scale array. *Mon. Wea. Rev.*, **107**, 1382–1387.

Ball, J. T., S. J. Thoren and M. A. Atwater, 1980: Cloud-coverage characteristics during Phase III of GATE as derived from satellite and ship data. *Mon. Wea. Rev.*, **108**, 1419–1429.

Brier, G. W., and J. Simpson, 1969: Tropical cloudiness and rainfall related to pressure and tidal variations. *Quart. J. Roy. Meteor. Soc.*, **95**, 120–147.

Brill, K., and B. Albrecht, 1982: Diurnal variations of the trade-wind boundary layer. *Mon. Wea. Rev.*, **110**, 601–613.

Browner, S. P., W. L. Woodley and C. G. Griffith, 1977: Diurnal oscillation of the area of cloudiness associated with tropical storms. *Mon. Wea. Rev.*, **105**, 856–864.

Cox, S. K., and K. T. Griffith, 1979: Estimates of radiative divergence during Phase III of the GARP Atlantic Tropical Experiment: Part II. Analysis of Phase III results. *J. Atmos. Sci.*, **36**, 586–601.

Dickson, R. A., 1979: Weather and circulation of November 1978. *Mon. Wea. Rev.*, **107**, 219–224.

Foltz, G. S., and W. M. Gray, 1979: Diurnal variation in the troposphere's energy balance. *J. Atmos. Sci.*, **36**, 1450–1466.

Fravalo, C., Y. Fouquart and R. Rosset, 1981: The sensitivity of a model of low stratiform clouds to radiation. *J. Atmos. Sci.*, **38**, 1049–1062.

Gray, W. M., and R. Jacobson, 1977: Diurnal variation of deep cumulus convection. *Mon. Wea. Rev.*, **105**, 1171–1188.

Griffith, C. G., W. L. Woodley, P. G. Grube, D. W. Martin, J. Stout and D. N. Sikdar, 1978: Rain estimation from geosynchronous imagery—Visible and infrared studies. *Mon. Wea. Rev.*, **106**, 1153–1171.

Gruber, A., 1976: An estimate of the daily variation of cloudiness over the GATE A/B area. *Mon. Wea. Rev.*, **104**, 1036–1039.

Hanson, H. P., and P. L. Gruber, 1982: Effect of marine stratocumulus clouds on the ocean-surface heat budget. *J. Atmos. Sci.*, **39**, 897–908.

Haragan, D. R., 1969: An investigation of clouds and precipitation for the Texas high plains. Texas Water Development Board, TDWR/R-111, 128 pp. [NTIS-PB297928].

Holle, R. L., and S. A. MacKay, 1975: Tropical cloudiness from all-sky cameras on Barbados and adjacent Atlantic Ocean. *J. Appl. Meteor.*, **14**, 1437–1450.

Howell, W. E., 1952: Local weather of the Chicama Valley (Peru). *Arch. Meteor. Geophys. Bioklim.*, **B5**, 41–53.

Jaffe, K. D., 1982: The diurnal cycle of summer convection over tropical Africa as determined from 1978 Meteosat satellite data. M.S. thesis, University of Washington, Seattle, 110 pp.

Kousky, V. E., 1980: Diurnal rainfall variation in northeast Brazil. *Mon. Wea. Rev.*, **108**, 488–498.

McGarry, M. M., and R. J. Reed, 1978: Diurnal variations in convective activity and precipitation during Phases II and III of GATE. *Mon. Wea. Rev.*, **106**, 101–113.

Minnis, P., and E. F. Harrison, 1984a: Diurnal variability of regional cloud and clear-sky radiative parameters derived from GOES data. Part I: Analysis method. *J. Climate Appl. Meteor.*, **23**, 993–1011.

——, and ——, 1984b: Diurnal variability of regional cloud and clear-sky radiative parameters derived from GOES data. Part III: November 1978 radiative parameters. *J. Climate Appl. Meteor.*, **23**, 1032–1051.

Paegle, J., and D. W. McLawhorn, 1983: Numerical modeling of diurnal convergence oscillations above sloping terrain. *Mon. Wea. Rev.*, **111**, 67–85.

Phillip, C. B., 1979: Observation of progressive convective interaction from the Rocky Mountain slopes to the plains. Atmos. Sci. Paper No. 316, Colorado State University, Ft. Collins, 100 pp. [ISSN 0067-0340].

Reed, R. J., and K. D. Jaffe, 1981: Diurnal variation of summer convection over West Africa and the tropical eastern Atlantic during 1974 and 1978. *Mon. Wea. Rev.*, **109**, 2527–2534.

Roach, W. T., R. Brown, S. J. Caughey, B. A. Crease and A. Slingo, 1982: A field study of nocturnal stratocumulus: I. Mean structure and budgets. *Quart. J. Roy. Meteor. Soc.*, **108**, 103–123.

Ruprecht, E., and W. M. Gray, 1976: Analysis of satellite-observed tropical cloud clusters. II. Thermal, moisture and precipitation. *Tellus*, **28**, 414–425.

Sadler, J. C., 1975: The upper tropospheric circulation over the global tropics. UHMET 75-05, University of Hawaii, 137 pp. [Available from the author at the University of Hawaii, Honolulu].

——, L. Oda and B. J. Kilonsky, 1976: Pacific ocean cloudiness from satellite observations. UHMET 76-01, University of Hawaii, 137 pp. [Available from the authors at the University of Hawaii, Honolulu].

Schubert, W. H., 1976: Experiments with Lilly's cloud-topped mixed layer model. *J. Atmos. Sci.*, **33**, 436–446.

——, J. S. Wakefield, E. J. Steiner and S. K. Cox, 1979: Marine stratocumulus convection. Part I: Governing equations and horizontally homogeneous solutions. *J. Atmos. Sci.*, **36**, 1286–1307.

Short, D. A., and J. M. Wallace, 1980: Satellite-inferred morning-to-evening cloudiness changes. *Mon. Wea. Rev.*, **108**, 1160–1169.

Simon, R. L., 1977: The summertime stratus over the offshore waters of California. *Mon. Wea. Rev.*, **105**, 1310–1314.

Trewartha, G. T., 1968: *An Introduction to Climate*. McGraw-Hill, 408 pp.

Virji, H., 1981: A preliminary study of summertime tropospheric circulation patterns over South America estimated from cloud winds. *Mon. Wea. Rev.*, **109**, 599–610.

Wallace, J. M., 1975: Diurnal variations in precipitation and thunderstorm frequency over the conterminous United States. *Mon. Wea. Rev.*, **103**, 406–419.

Weickmann, H. K., A. B. Long and L. R. Hoxit, 1977: Some examples of rapidly growing oceanic cumulonimbus clouds. *Mon. Wea. Rev.*, **105**, 469–476.